



## ORIGINAL ARTICLE

# Folding correction of ABC-transporter ABCB1 by pharmacological chaperones: a mechanistic concept

Matthias Spork<sup>1</sup>, Muhammad Imran Sohail<sup>1,2</sup>, Diethart Schmid<sup>3</sup> , Gerhard F. Ecker<sup>4</sup>, Michael Freissmuth<sup>5</sup>, Peter Chiba<sup>1</sup>  & Thomas Stockner<sup>5</sup>

<sup>1</sup>Institute of Medical Chemistry, Center of Pathobiochemistry and Genetics, Medical University of Vienna, Waehringerstrasse 10, Vienna A-1090, Austria

<sup>2</sup>Department of Zoology, Government College University Lahore, Katchery Road, Lahore 54000, Pakistan

<sup>3</sup>Institute of Physiology, Center of Physiology und Pharmacology, Medical University of Vienna, Schwarzspanierstrasse 17, Vienna A -1090, Austria

<sup>4</sup>Department of Medicinal Chemistry, University of Vienna, Emerging Field Pharmacoinformatics, Althanstrasse 14, Vienna A-1090, Austria (GFE)

<sup>5</sup>Institute of Pharmacology, Center of Physiology und Pharmacology, Medical University of Vienna, Waehringerstrasse 13a, Vienna A-1090, Austria

## Keywords

ABC transporter, folding correction, P-glycoprotein, pharmacochaperone

## Correspondence

Peter Chiba, Institute of Medical Chemistry, Center for Pathobiochemistry and Genetics, Medical University of Vienna, Waehringerstrasse 10, A-1090 Vienna, Austria. Tel: +43 1 40160 38005; Fax: +43 1 40160 938081; E-mail: peter.chiba@meduniwien.ac.at

## Funding Information

This research was supported by grants from the Austrian Science Fund FWF (APF03509FW) within the scope of SFB35 (P.C., G.E., M.F., T.S.). MIS is a scholarship recipient of the Higher Education Commission Pakistan.

Received: 23 September 2016; Accepted: 21 March 2017

*Pharma Res Per*, 5(3), 2017, e00325, doi: 10.1002/prp2.325

doi: 10.1002/prp2.325

## Introduction

ATP-binding cassette (ABC) proteins are found in all kingdoms of life and thus form one of the largest protein families (Rees et al. 2009). In humans 48 genes code for ABC proteins, the majority of which are transmembrane

## Abstract

Point mutations of ATP-binding cassette (ABC) proteins are a common cause of human diseases. Available crystal structures indicate a similarity in the architecture of several members of this protein family. Their molecular architecture makes these proteins vulnerable to mutation, when critical structural elements are affected. The latter preferentially involve the two transmembrane domain (TMD)/nucleotide-binding domain (NBD) interfaces (transmission interfaces), formation of which requires engagement of coupling helices of intracellular loops with NBDs. Both, formation of the active sites and engagement of the coupling helices, are contingent on correct positioning of ICLs 2 and 4 and thus an important prerequisite for proper folding. Here, we show that active site compounds are capable of rescuing P-glycoprotein (P-gp) mutants  $\Delta Y490$  and  $\Delta Y1133$  in a concentration-dependent manner. These trafficking deficient mutations are located at the transmission interface in pseudosymmetric position to each other. In addition, the ability of propafenone analogs to correct folding correlates with their ability to inhibit transport of model substrates. This finding indicates that folding correction and transport inhibition by propafenone analogs are brought about by binding to the active sites. Furthermore, this study demonstrates an asymmetry in folding correction with cis-flupentixol, which reflects the asymmetric binding properties of this modulator to P-gp. Our results suggest a mechanistic model for corrector action in a model ABC transporter based on insights into the molecular architecture of these transporters.

## Abbreviations

ABC, ATP-binding cassette; HEK293, human embryonic kidney 293 cells; ICL, intracellular loop; MDR, multidrug resistance; NBD, nucleotide-binding domain; P-gp, P-glycoprotein; rh123, rhodamine123; TMD, transmembrane domain.

transporters. Some members of the human ABC protein family are not involved in active transport, but function in mediating ion conductance or ion channel regulation. Transporters recognize a diverse panel of cargo molecules including lipids, drugs, cyclic nucleotides, nucleobases, and bile acids. Dysfunction of at least 22 human ABC

transporters has been linked to more than 27 disease etiologies (Chiba et al. 2014). Tangier disease (ABCA1), progressive familial intrahepatic cholestasis type 3 (ABCB4) and type 2 (ABCB11), Dubin-Johnson syndrome (ABCC2), pseudoxanthoma elasticum (ABCC6), general arterial calcification of infancy (ABCC6), cystic fibrosis (ABCC7), hyperinsulinemic hypoglycemia of infancy (ABCC8), and gout (ABCG2) are important examples of diseases caused by impairment of ABC proteins. Point mutations, which lead to folding deficiency, are a major cause of diseases associated with ABC proteins. Among them cystic fibrosis is the most frequent with an incidence of approximately 1 in 3500 births in Austria (Farrell 2008).

Several members of the human ABC family are involved in drug disposition. The most intensely studied human multidrug ABC transporter is P-glycoprotein (P-gp), also referred to as MDR1 or ABCB1. It exports a diverse panel of structurally and functionally unrelated cytostatic drugs, thereby rendering human cancer cells multidrug resistant. We selected this multidrug transporter as a model system for studying folding because of its ability to interact with a large complement of small molecular weight compounds. This increases the likelihood of identifying active compounds. The mutants ABCB1- $\Delta$ Y490 (Hoof et al. 1994), a mutation located in the first alpha helix of the alpha helical domain of NBD1 (recently named the E-helix in inverted subfamily G transporters) (Lee et al. 2016), and ABCB1- $\Delta$ Y1133, its analogous mutation in NBD2, were used in these experiments because amino acid residues in this alpha helix contribute to the ball and socket interaction of ICLs 2 and 4 with the NBDs (Jin et al. 2012). Furthermore, Y490 is the analogous position of F508 in the cystic fibrosis transmembrane conductance regulator (CFTR, ABCC7) (Hoof et al. 1994). Deletion of this residue ( $\Delta$ F508), the most prevalent mutation in cystic fibrosis, is found in at least one allele in 90% of all patients (Kerem et al. 1989; Riordan et al. 1989). The  $\Delta$ Y490 and  $\Delta$ Y1133 mutants are representative for frequent other mutations in their vicinity with respect to their position in the alpha helical domain. These include mutations in the breast cancer-related protein (ABCG2, a major contributor to gout particularly in the Japanese population) (Matsuo et al. 2009), the cholesterol transporter (ABCA1) (Bodzioch et al. 1999; Rust et al. 1999), and the conjugated bilirubin transporter (ABCC2).

Propafenone analogs were extensively characterized by our group in the past and found to be both, substrates and inhibitors of P-gp (Chiba et al. 1995; Schmid et al. 1999). Active sites were characterized by photolabeling and subsequent identification of ligand-modified

component peptide fragments by mass spectrometry (Pleban et al. 2005; Parveen et al. 2011). ABCB1 is considered to have arisen from a homodimeric ancestor by gene duplication (Gottesman and Pastan 1993). We found that binding of propafenones occurs at the transmembrane domain interface in either of two modes, which are related to each other by pseudosymmetry. During photolabeling the photoactive arylketone group of propafenones is oriented toward the helix 5/8 and 2/11 interfaces respectively. Residues in the latter contribute to the preferred binding mode 2 of these compounds (Parveen et al. 2011). Active site tyrosine residue 953 was identified to contribute to propafenone binding in mode 2 (Donmez Cakil et al. 2014). Previous data demonstrated that substrates and inhibitors of P-gp can act as pharmacological chaperones by promoting folding of trafficking deficient mutants (Loo and Clarke 1997, 1998, 2013, 2014; Loo et al. 2005). Therefore, we examined the rescue of P-gp transmission interface mutants  $\Delta$ Y490 and  $\Delta$ Y1133 with propafenone analogs, which bind to active sites at the TMD interface, and also with cis-flupentixol, an allosteric modulator of P-gp, interaction of which is restricted to TMD2 only. The prediction was that propafenones ought to rescue both mutants, while the rescuing effect of cis-flupentixol ought to be asymmetric. Indeed such an asymmetry was found. This finding allowed for the development of a mechanistic concept for pharmacochaperone action.

## Materials and Methods

### Knockdown of endogenous P-gp in human embryonic kidney 293 cells

Human embryonic kidney 293 (HEK293) cells express endogenous P-gp, which compromises the quantification and functional characterization of transiently expressed P-gp mutants. Thus, the endogenous protein was knocked down by transduction with pLKO.1 lentiviral vectors containing P-gp small hairpin (shRNA) constructs targeted to the 3' untranslated region of the gene as described previously (Donmez Cakil et al. 2014).

### Construction of mutants

Mutants  $\Delta$ Y490 and  $\Delta$ Y1133 of hexa-his-tagged human P-gp were generated in the entry vector pENTR4 (Invitrogen, Carlsbad, CA). The following forward and reverse primers were used (Microsynth, Wolfurt, Austria):  $\Delta$ Y490-forw 5'- GCT GAA AAC ATT CGC GGC CGT GAA AAT GTC -3';  $\Delta$ Y490-rev 5'- GAC ATT TTC ACG GCC GCG AAT GTT TTC AGC -3';  $\Delta$ Y1133-forw 5'- GCT GAG AAC ATT GCC GGA GAC

AAC AGC CGG -3';  $\Delta$ Y1133-rev 5'- CCG GCT GTT GTC TCC GGC AAT GTT CTC AGC -3'; For transfer of P-gp constructs from entry vector pENTR4 into the proprietary gateway compatible destination vector pCEP4d, the unique recombination properties of bacteriophage lambda attL and attR sites were used as described (Hartley et al. 2000).

### Expression of P-gp in HEK293 cells

Transient transfection of HEK293 cells with wild-type or mutant P-gp was performed as described previously (Donmez Cakil et al. 2014) using TurboFect transfection reagent (Fisher Scientific, Vienna, Austria).

### Rhodamine123 efflux assay

Rhodamine123 (rh123) efflux assays with transiently transfected HEK293 cells were performed after a 24 h incubation at 28°C or 37°C. Cells were harvested by trypsinization after washing with phosphate-buffered saline (PBS), and centrifuged at 500 g followed by resuspension of the pellet with DMEM (pH 7.8) containing rh123 (Sigma Chemical Co., St. Louis) at a final concentration of 0.2  $\mu$ g/mL (0.53  $\mu$ mol/L). Loading with rh123 was carried out in a water bath under continuous shaking at 37°C for 30 min. Afterwards cell were chilled on ice and subsequently washed with ice-cold DMEM (pH 7.4) to remove extracellular rh123. Cell pellet was resuspended in DMEM at 37°C (pH 7.4) to start efflux of rh123. The cellular fluorescence was continuously monitored in a Becton Dickinson FACSCalibur flow cytometer (BD Biosciences, Vienna, Austria) and the first order rate constants (*k*-values) were calculated as described previously (Donmez Cakil et al. 2014).

### Daunomycin efflux inhibition assay

CCRFvcr1000 cells were loaded with daunomycin (Sigma Chemical Co., St. Louis) in RPMI1640 media (pH 7.8) at a final concentration of 1.69  $\mu$ g/mL (3.0 mol/L), as described for rh123 efflux assay. After washing with ice-cold RPMI1640 (pH 7.4), cells were resuspended in RPMI1640 media prewarmed to 37°C (pH 7.4) containing either solvent or compound. Eight concentrations (serial 1:3 dilution) were tested for each potential inhibitor. The excitation wavelength for daunomycin was 488 nm and emission was monitored with a 585/42 nm band-pass filter (FL2). The efflux was measured with a FACSCalibur and IC<sub>50</sub> values were calculated as outlined previously (Donmez Cakil et al. 2014).

### Quantification of surface expression by indirect immunofluorescence

Transiently transfected cells were cultured at either 28 or 37°C for 24 h for temperature shift experiments. For pharmacochaperone experiments, cells were incubated with compounds or solvent for 24 h at 37°C. Eight concentrations were tested for each compound ranging from 195 nmol/L to 25 mol/L. Subsequently, cells were harvested by trypsinization, washed with PBS, and incubated for 30 min with the primary mouse monoclonal anti-P-gp antibody MRK16 (final concentration: 5  $\mu$ g/mL) (Kamiya Biomedical Company, Seattle, WA) or IgG2a control antibody (final concentration: 2.5  $\mu$ g/mL) (BD Biosciences, Vienna, Austria). Cells were again washed with PBS and incubated with FITC-labeled goat antimouse antibody (final concentration: 12.5  $\mu$ g/mL) (BD Biosciences, Vienna, Austria) for 30 min in the dark at 2–8°C in a cold room. Thereafter, the cells were washed with PBS and resuspended. A Becton Dickinson FACSCalibur flow cytometer was used to measure MDR1 surface expression (Fig. 3A, B). The excitation wavelength was 488 nm and emission was monitored with a 530/30 nm band-pass filter (FL1). The EC<sub>50</sub> values for individual compounds were calculated by fitting data points for P-gp surface expression to the equation of a saturation hyperbola by nonlinear regression.

### Compounds

Cyclosporin A was purchased from Fluka (Sigma Chemical Co., MO). cis-Flupentixol was a generous gift from Saibal Dey. Propafenones were synthesized as described (Chiba et al. 1995). The structures of propafenone analogs are shown in Table 1. Their authenticity was verified by <sup>1</sup>H and <sup>13</sup>C-NMR.

### Homology modeling

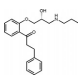
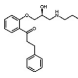
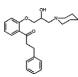
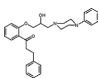
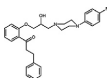
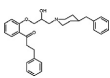
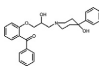
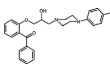
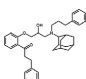
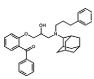
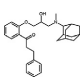
The ABCB1 homology model was generated as described previously (Stockner et al. 2009). The model of human P-gp is based on the crystal structure of *M. musculus* P-gp (PDB ID: 4XWK) (Nicklisch et al. 2016).

### Results

#### Selection of P-gp transmission interface mutants

Crystal structures of several prokaryotic and mammalian ABC exporters share a common architecture, in which each TMD forms contacts with both NBDs via segments, which are referred to as coupling helices. Thereby partially domain-swapped TMD/NBD interfaces (also

**Table 1.** Structures of propafenone analogs.

Compound	Chemical structure	Molecular mass	IC <sub>50</sub> of daunomycin transport inhibition Mean ± SD (mol/L)	EC <sub>50</sub> for rescue of ΔY490 Mean ± SD (mol/L)	EC <sub>50</sub> for rescue of ΔY1133 Mean ± SD (mol/L)	REFERENCE
(R)-propafenone		341.44	0.234 ± 0.038	32.63 ± 0.14	37.54 ± 4.77	(Chiba <i>et al.</i> 1998)
(S)-propafenone		341.44	0.242 ± 0.025	35.95 ± 1.51	40.49 ± 5.52	(Chiba <i>et al.</i> 1998)
GPV005		367.48	0.251 ± 0.031	39.39 ± 3.66	38.51 ± 0.60	(Langer <i>et al.</i> 2004)
GPV019		444.57	0.493 ± 0.056	86.36 ± 2.70	89.18 ± 1.23	(Langer <i>et al.</i> 2004)
GPV031		462.56	0.068 ± 0.014	7.03 ± 0.67	5.66 ± 0.85	(Langer <i>et al.</i> 2004)
GPV128		457.60	0.029 ± 0.003	4.01 ± 0.74	4.08 ± 0.17	(Langer <i>et al.</i> 2004)
GPV317		431.52	0.211 ± 0.015	33.65 ± 0.66	38.38 ± 3.23	(Langer <i>et al.</i> 2004)
GPV319		434.50	0.180 ± 0.019	29.43 ± 6.12	25.67 ± 3.72	(Langer <i>et al.</i> 2004)
GPV982		551.76	0.157 ± 0.034	24.92 ± 1.11	26.42 ± 0.27	
GPV984		523.70	0.222 ± 0.021	29.22 ± 3.94	30.31 ± 4.43	
GPV987		447.61	0.068 ± 0.006	10.87 ± 1.57	11.76 ± 2.60	

referred to as transmission interfaces) are formed, which function in propagating conformational changes from the NBDs to the TMDs and vice versa. These transmission interfaces are frequently targeted by disease-causing mutations that lead to improper protein folding and subsequent trafficking deficiency (Hashimoto *et al.* 2002; Imai *et al.* 2002; Hirouchi *et al.* 2004; Tornovsky *et al.* 2004; Hayashi *et al.* 2005; Cheong *et al.* 2006; Singaraja *et al.* 2006; Le Saux *et al.* 2011; Gautherot *et al.* 2012; Sorrenson *et al.* 2013). A systematic review of the literature for

naturally occurring single nucleotide polymorphisms (SNPs) and single amino acid deletions was performed. We identified 126 confirmed trafficking deficient mutations in 12 different ABC proteins from four subfamilies. For an alignment of full-length transporters and homodimeric half transporters, sequences of the latter were duplicated. We were able to assign positions of 85 mutations to the ABCB1 protein sequence. For the ABCA subfamily an alignment of the TMDs was compromised because secondary structure analyses show large





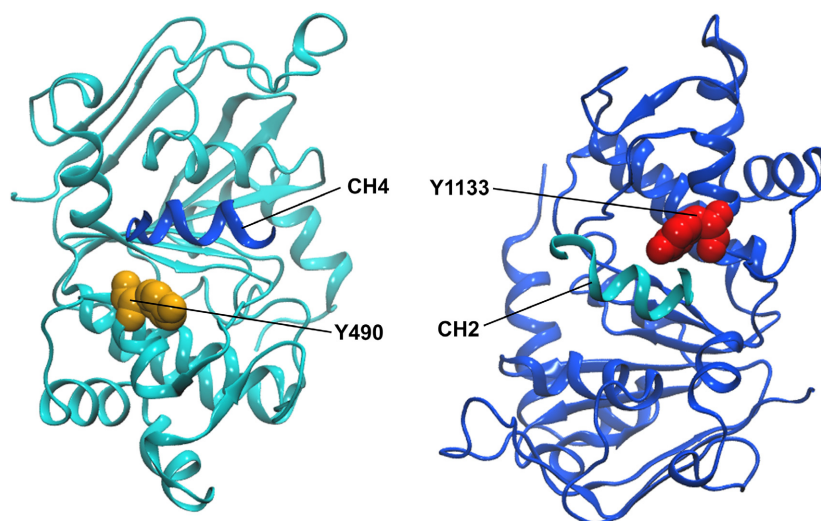


**Figure 2.** The positions of tyrosine 490 in NBD1 (orange), tyrosine 1133 in NBD2 (red), and coupling helices (CH) of ICLs2 and 4 (CH2, CH4) are depicted in a homology model of human P-gp (template *M. musculus* P-gp (PDB ID: 4XWK)). The N-terminal half of the protein is colored in cyan, the C-terminal half is depicted in dark blue.

dihydrochloride, a first pharmacological chaperone for the treatment of phenylketonuria, has been introduced in the market in the United States in 2007 (Thompson 2008), thus providing a proof of principle that folding correction by pharmacochaperones is a valid therapeutic approach. The concept of folding correction with small molecules is also supported by several in vitro studies on members of the ABC-transporter family (Polgar et al. 2004; Loo et al. 2005; Pedemonte et al. 2005; Iram and Cole 2012). Importantly, treatment with pharmacological chaperones would only be considered successful if the rescued mutants were still functional. In order to test if transmission interface mutants  $\Delta Y490$  and  $\Delta Y1133$  were functional when expressed at the plasma membrane, a temperature shift to 28°C was used to promote maturation of the nascent protein (Machamer and Rose 1988). Thermal rescue of folding deficiency has been amply demonstrated and was also specifically reported for human ABC family members (Denning et al. 1992; Loo and Clarke 1994; Plass et al. 2004; Delaunay et al. 2009). Plasma membrane expression levels and first-order rate constants for rh123 transport were determined 24 h after shifting cells to 28°C. Expression of mutants  $\Delta Y490$  and  $\Delta Y1133$  increased by a factor of  $3 \pm 1$  and  $11 \pm 4$  ( $n \geq 3$ ), respectively. Figure 4 shows transport rates as a function of surface expression. For any transporter a linear relationship between these parameters is obtained as long as its function is not impaired. For transport-deficient mutants slopes were lower than that for wild-type protein. Data points for wild-type P-gp and the  $\Delta Y490$

mutant were found to be located on the same line, indicating that the mutant is functional once it reaches the plasma membrane. For the  $\Delta Y1133$  mutant low expression levels precluded a definitive statement about its functionality (Fig. 4).

### Rescue of P-gp mutants with propafenones

We extensively characterized propafenone analogs in the past with respect to their properties as both substrates and inhibitors of P-gp (Chiba et al. 1995; Schmid et al. 1999). Previous studies on P-gp revealed that substrates and inhibitors can act as pharmacological chaperones (Loo and Clarke 1997, 1998, 2013, 2014; Loo et al. 2005). More than 60 propafenone analogs were screened at three concentrations (0.25, 2.5, and 25 mol/L) and 11 of those were found to be active at least at the highest concentration used (data not shown). For active compounds full concentration–response curves were obtained. Figure 5 shows a comparison of the rescue potential in the two mutants for these 11 propafenone analogs. Chemical structures of those compounds are shown in Table 1. Cyclosporin A was used as a reference pharmacological chaperone (Loo and Clarke 1997).  $EC_{50}$  values were calculated by nonlinear regression. Almost identical  $EC_{50}$  values for these compounds were obtained for both mutants ( $R^2 = 0.99$ ) (Fig. 5). Thus, propafenones have the capacity to rescue folding of P-gp transmission interface mutants. Rescue is concentration dependent and similar for both the  $\Delta Y490$  and  $\Delta Y1133$  mutant.

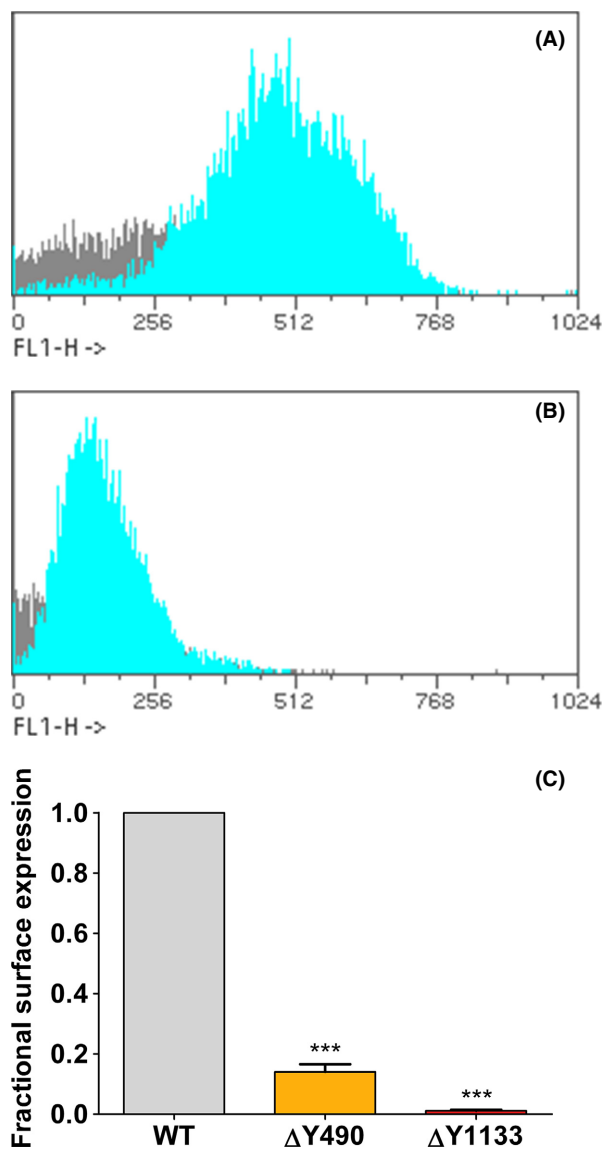


**Figure 3.** (A) Representative histogram of the surface expression of wild-type (WT) protein. The MRK16 antibody was used as the primary antibody. FITC-conjugated goat antimouse antibody was used as the secondary antibody. Fluorescence was measured in a FACSCalibur flow cytometer as described in detail in the methods section. The abscissa shows mean fluorescence intensities (as channel numbers) in FL1. Viable cells are indicated in cyan. The arithmetic mean of the population was determined. From this, the mean fluorescence units per cell were calculated. The latter are a relative measure of P-gp surface expression. (B) Same as A, but for mutant  $\Delta Y1133$ . (C) Bar graph showing the fractional surface expression of P-gp interface mutants in comparison with wild-type (WT) protein. Surface expression was determined by indirect immunostaining with the MRK16 antibody using flow cytometry and normalized to surface expression of WT protein. Means  $\pm$  S.D. from seven independent experiments were compared using one-way ANOVA. Post hoc Tukey analyses were performed to find groups with significantly different mean values. Significantly different from wild type: \*\*\* $P < 0.001$ .

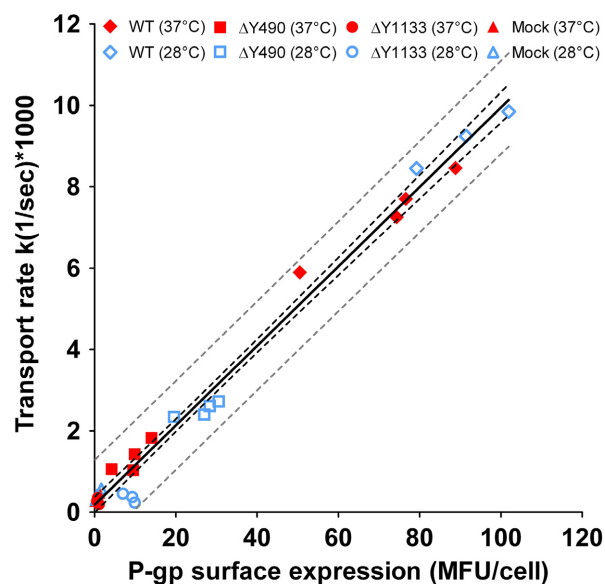


**Figure 4.** A total of 27 efflux experiments are shown. Data points represent the mean of duplicate determinations. First-order rate constants of rh123 transport are plotted as a function of P-gp surface expression (determined by indirect immunostaining with the MRK16 antibody). The square of the correlation coefficient is 0.99 with a  $P < 0.001$ . A linear regression fit, the 99% confidence interval (black dashed lines), and 99% prediction interval (grey dashed lines) are indicated.

### IC<sub>50</sub> values for daunomycin transport inhibition and EC<sub>50</sub> values for trafficking rescue correlate

As previously shown by photolabeling, propafenone-binding sites are located at the TMD/TMD interface (Pleban et al. 2005) at a distance of more than 60 Å from the sites of mutation (Fig. S2). Propafenones are substrates of P-gp and thus also act as competitive inhibitors of other substrates. Binding to active sites can thus be monitored by determining IC<sub>50</sub> values. If binding to the active sites indeed mediated both the inhibitory and the pharmacochaperone effect of the compound class, a correlation between IC<sub>50</sub> and EC<sub>50</sub> values would be expected in a larger set of compounds. Therefore, 11 compounds, which were identified as folding correctors, were also evaluated for P-gp inhibitory activity. Figure 6 shows the correlation for mutant  $\Delta Y490$ . The  $R^2$  value was found to be 0.98. Thus, it is safe to infer that the effect of propafenones to correct folding is mediated by their binding to active sites through a long-range effect.

### Rescue of interface mutants with allosteric P-gp modulator cis-flupentixol

It has been demonstrated by several lines of evidence that substrates and several small molecule inhibitors bind to

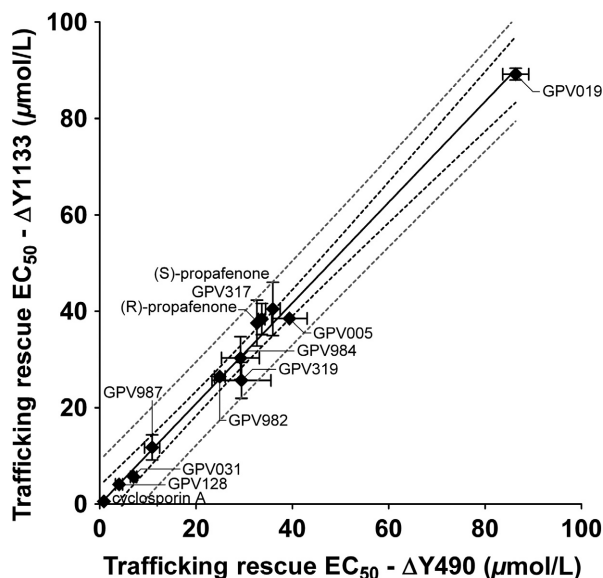


**Figure 5.** Correlation between  $EC_{50}$  values for trafficking rescue of mutants  $\Delta Y1133$  and  $\Delta Y490$ .  $EC_{50}$  values were calculated by nonlinear regression analysis of concentration response curves. The square of the correlation coefficient is 0.99 with a  $P < 0.001$ . A linear regression fit minimizing sum of squares, the 99% confidence interval (black dashed lines), and 99% prediction interval (grey dashed lines) are displayed. Mean  $\pm$  S.D. of at least two independent experiments.

the TMD interface of P-gp. The evidence is as follows: (1) refined structures of mouse P-gp show the cyclic QZ peptide inhibitors in different positions along the interface. (2) Propafenones photolabel the TM helix 5/8 interface and in pseudosymmetric position helix 11, which contacts helix 2 of TMD1. (3) The majority of residues that have been identified in mutation analyses are predicted to be located at the interface in P-gp homology models. Therefore, we tried to identify a compound, binding properties of which are restricted to one TMD only. The underlying hypothesis posited asymmetric rescue of such a compound. *cis*-Flupentixol fulfills these criteria based on the amino acid residues in P-gp, which are important for mediating the allosteric effects of *cis*-flupentixol on substrate binding and ATPase activity (Mandal et al. 2012). A projection of these residues into a homology model of human P-gp based on the mouse structure (Nicklisch et al. 2016) is shown in Figure 7A, B. These residues are exclusively located in TMD2.  $EC_{50}$  values for trafficking rescue were determined and found to be as follows:  $\Delta Y490$   $8.7 \pm 1.8$  mol/L; mutant  $\Delta Y1133$ :  $31 \pm 4.4$  mol/L. Thus, the  $EC_{50}$  value is almost fourfold higher for the NBD2 than for the NBD1 mutant. This strongly contrasts with results obtained for propafenones and cyclosporin A (Fig. 7C, D).

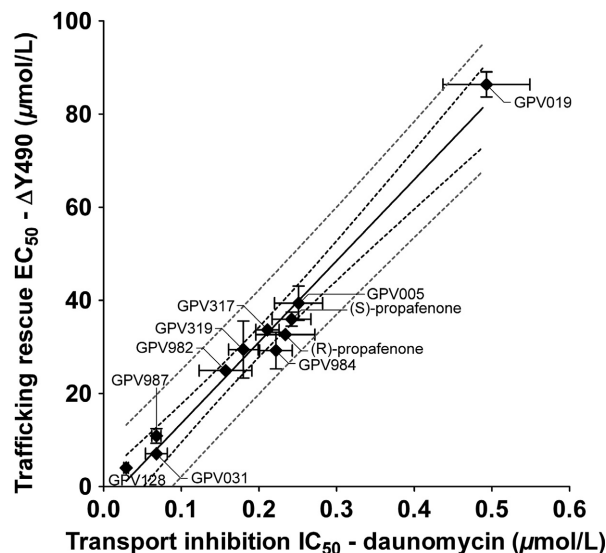


**Figure 6.** Correlation between  $EC_{50}$  values for trafficking rescue and  $IC_{50}$  values for daunomycin transport inhibition. The square of the correlation coefficient is 0.98 with a  $P < 0.001$ . A linear regression fit minimizing sum of squares, the 99% confidence interval (black dashed lines), and 99% prediction interval (grey dashed lines) are shown. Mean  $\pm$  S.D. from at least two independent experiments.

## Discussion

Correct positioning of ICLs can be considered a prerequisite for engagement of the TMD coupling helices with membrane-oriented NBD surfaces. This domain interaction leads to formation of the TMD/NBD transmission interfaces, which represent a critical element for the adoption of a fully folded conformation. Clustering of mutations at these interfaces is observed across different subfamilies and members of the human ABC protein family. The cystic fibrosis transmembrane conductance regulator CFTR is a chloride channel, deficiency of which gives rise to cystic fibrosis, the most frequently lethal inherited disease in humans. The paradigmatic  $\Delta F508$  mutation, which is observed in at least one allele in 90% of patients, conforms to mutant  $\Delta Y490$  in NBD1 of human P-gp. Folding deficiency of this mutant has been identified as the root cause in this and a number of other mutants. The corresponding position of residue Y490 in NBD2 is Y1133 (Figs. 1, 2 and S1A, B). Deletion of residue Y1133 compromises folding more severely than that of residue Y490 (Fig. 3C). Our finding is in accordance with earlier data by Loo and Clarke indicating that mutations in analogous positions of the two transmission interfaces affect P-gp folding differentially and more severely, when mutations are located in NBD2 (Wang et al. 2007). In particular these authors demonstrated that coupling helices 2 and 3 and adjacent portions of ICLs 2



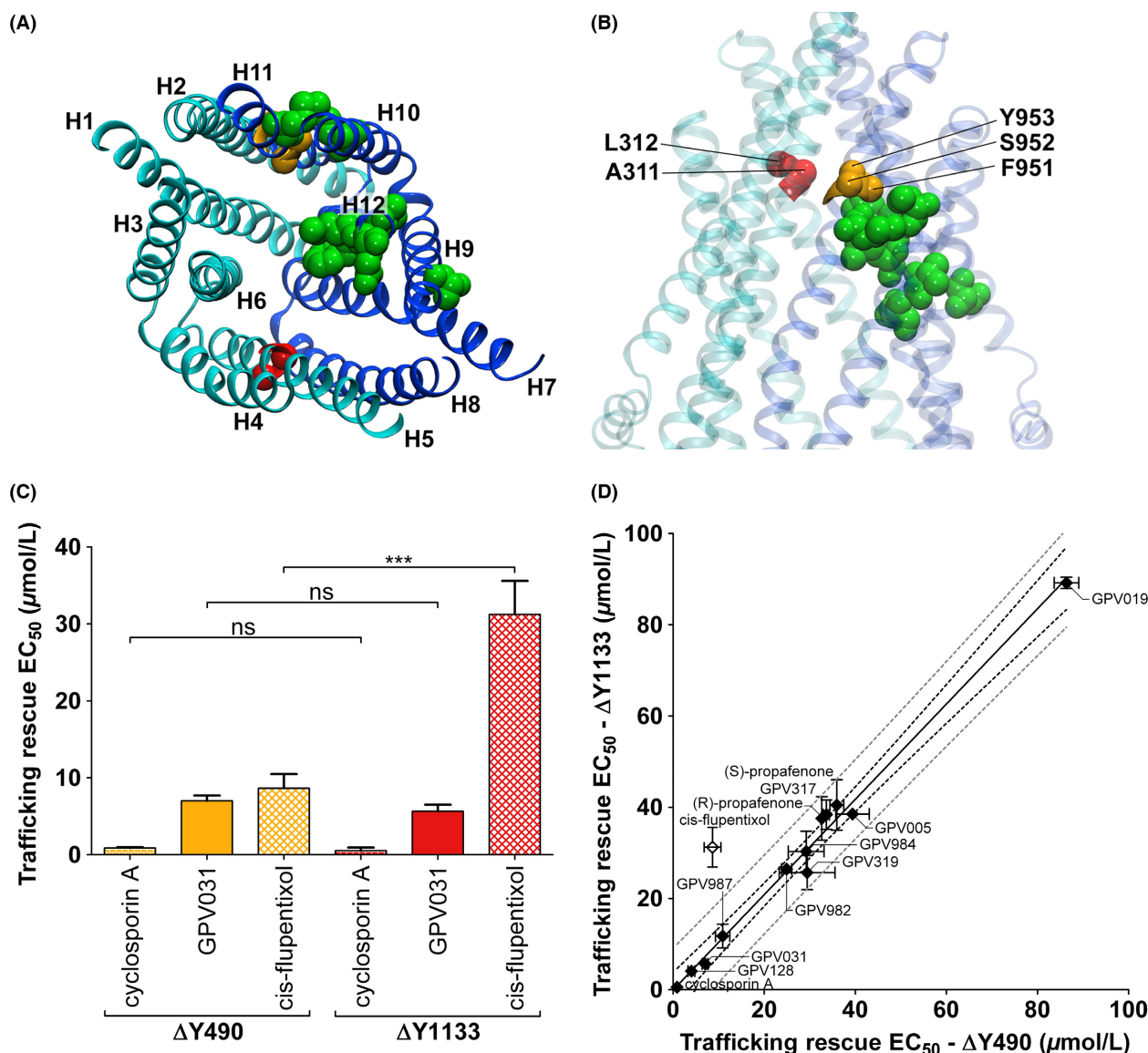


**Figure 7.** Homology model of human P-gp (template *M. musculus* P-gp (PDB ID: 4XWK)) indicating locations of residues involved in cis-flupentixol binding (green) as well as  $\alpha$ -C-atoms of residues at the TMD/TMD interface, which were previously found to be labeled by propafenones (red: A311, L312) (orange: F951, S952, Y953). The N-terminal half of the protein is colored in cyan, the C-terminal half is colored in dark blue. (A) Bottom view. (B) Side view. (C) Bar graph showing  $EC_{50}$  values for trafficking rescue of  $\Delta Y490$  (orange) and  $\Delta Y1133$  (red) with cyclosporin A, GPV031, and cis-flupentixol.  $EC_{50}$  values were calculated by nonlinear regression analysis of concentration response curves. Means  $\pm$  S.D. from at least three independent experiments were compared using one-way ANOVA. Post hoc Tukey analyses were performed to find groups with significant different mean values. (D) Graph showing  $EC_{50}$  values for trafficking rescue of mutant  $\Delta Y1133$  in correlation with trafficking rescue  $EC_{50}$  values for trafficking rescue of mutant  $\Delta Y490$ . A linear regression fit minimizing sum of squares, the 99% confidence interval (black dashed lines), and 99% prediction interval (grey dashed lines) are shown. Mean  $\pm$  S.D. from at least two independent experiments.

and 3 are more sensitive to point mutations than coupling helices 1 and 4 and adjacent portions of ICLs 1 and 4 (Loo et al. 2013; Loo and Clarke 2015).

Temperature shift experiments indicated that surface expression of both mutants was increased at lower temperature thus indicating the possibility for

thermodynamic stabilization (Fig. 4). Several substrates/inhibitors of P-gp can elicit a similar effect and therefore act as pharmacological chaperones. This has been shown previously for cyclosporin A, vinblastine, verapamil, and capsaicin (Loo and Clarke 1997, 1998, 2013, 2014; Loo et al. 2005). This evidence led us to explore the ability of

the class of propafenone derivatives to act as pharmacological chaperones. Indeed, a number of compounds were able to increase surface expression in a concentration-dependent manner with similar  $EC_{50}$  values for both mutants (Fig. 5). Our observations identified propafenone analogs as potent pharmacological chaperones with  $EC_{50}$  values of selected compounds in the low micromolar range.

The binding modes of propafenone analogs were previously characterized using photolabeling and mass spectrometry. These studies revealed two binding modes at the TMD interface, which are related to each other by pseudosymmetry (Pleban *et al.* 2005; Parveen *et al.* 2011). The two positively cooperative binding sites for rhodamine123 and Hoechst33342, named R- and H-sites by Shapiro and Ling (Shapiro and Ling 1997) after their eponymous substrates, may relate to a preference for one of these two binding modes. The distance between the photolabeled active site residues in the apex of the central cavity and the positions of mutations at the transmission interface can be estimated in different crystal structures of ABC transporters and homology models of human P-gp to be more than 60 Å (Fig. S2). We thus addressed the question, if a long-range effect was responsible for folding correction. A correlation between  $IC_{50}$  values for transport inhibition and  $EC_{50}$  values was found for a larger set of propafenone analogs (Fig. 6). This correlation makes it likely that rescue is indeed brought about by a long-range effect.

In order to achieve their native conformation, proteins have to undergo cotranslational and posttranslational folding. As shown for CFTR, proteins first attain a loosely folded conformation (Kleizen *et al.* 2005), which subsequently is compacted when interdomain interfaces are formed. This cooperative posttranslational domain assembly is required for stabilization of protein domains, absence of which represents a root cause for global misfolding and impaired trafficking ensuing from point mutations (Du and Lukacs 2009). Accordingly, deletion of residue F508 does not only affect the conformational stability of NBD1 but also disturbs the stability of TMD1, TMD2, and NBD2, as shown by limited proteolysis (Rabeh *et al.* 2012). Stabilization of TMDs through interaction with NBD1 is crucial for the rescue of CFTR mutant  $\Delta F508$  (Rabeh *et al.* 2012). Thus, cooperative domain folding is likely to also contribute to domain assembly of other ABC transporters (Du and Lukacs 2009). In light of this model we postulate the following mechanism for trafficking rescue of ABCB1 with active site compounds (Fig. 8): in the absence of pharmacological chaperones (Fig. 8A) only wild type attains its fully folded conformation (right, boxed in green), while the mutants reach an end point of folding, which lies outside the proteostasis boundary (boxed in red). In the presence of propafenones, folding of both mutants is corrected (Fig. 8B). *cis*-Flupentixol rescues mutant  $\Delta Y1133$  to a lesser extent than mutant  $\Delta Y490$  as evidenced by an almost fourfold higher  $EC_{50}$  value

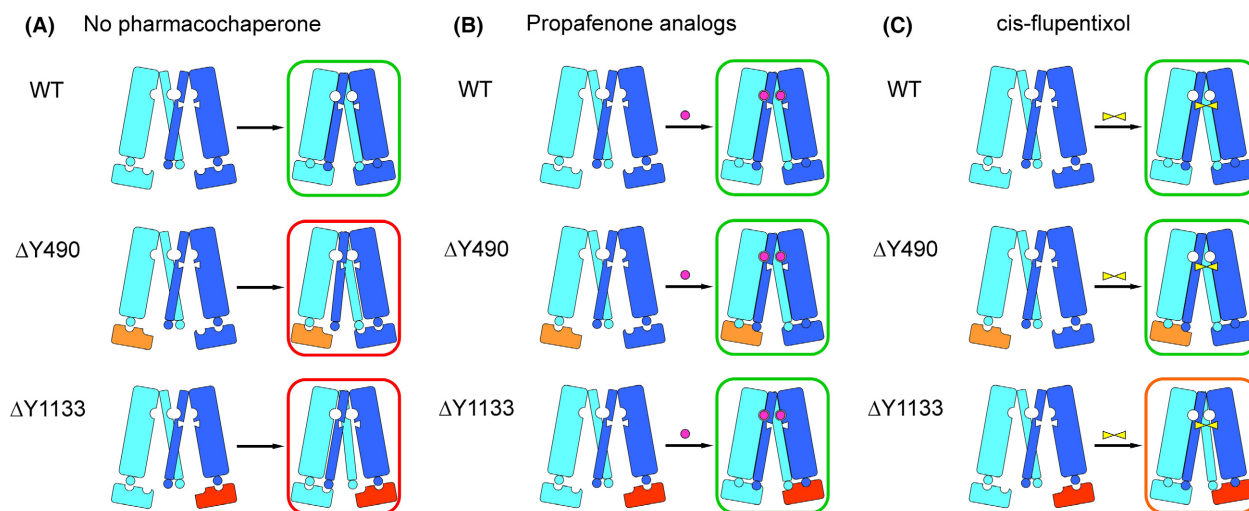


**Figure 8.** Cartoons displaying the posttranslational domain assembly of wild-type P-gp and transmission interface mutants  $\Delta Y490$  (NBD1: orange) and  $\Delta Y1133$  (NBD2: red). The N-terminal half of P-gp is colored in cyan, the C-terminal half in dark blue. Starting points prior to domain assembly are depicted on the left and folding end points are shown on the right. (A) In the absence of pharmacochaperones only wild-type P-gp reaches a fully folded conformation (green box), whereas interface mutants remain outside the proteostasis boundary (red boxes). (B) Treatment with propafenone analogs (purple circles) results in a fully folded conformation in wild type and mutants (green boxes). (C) *cis*-Flupentixol (yellow bow tie symbol) rescues folding of mutant  $\Delta Y490$  (green box), whereas mutant  $\Delta Y1133$  can only be rescued partially (orange box).

(Fig. 7C, D). A partial rescue is accounted for by the cooperative nature of domain assembly (framed in orange) (Fig. 8C). Hence, mutation-induced conformational changes in one domain compromise domain interplay on more general terms. Active site compounds contribute an energetic term by selecting conformations of an a priori flexible domain, which have an increased propensity to interact with their congeneric partner domain(s). In the case of ABC proteins and propafenones, this would result in an increased probability of one TMD to interact with the other. This model is consistent with the concept laid out in the conformational selection principle (Changeux *et al.* 1967; Burgen 1981). Mechanistically, this implies that small molecular weight ligands first interact with one TMD and this intermediate forms a ternary complex with the other TMD. The nascent conformation initially lacks cross-domain interactions thus requiring much higher concentrations of compounds for pharmacochaperone activity than for transport inhibition. Indeed, the approximately 160-fold higher concentration required for folding correction supports this notion (Fig. 6).

In contrast to competitive inhibitors, *cis*-flupentixol has been reported to prevent translocation and subsequent dissociation of radiolabeled P-gp substrate iodoarylazidoprazosin without competing for binding to the active sites (Maki *et al.* 2003; Maki and Dey 2006). Multiple sequence alignments of mammalian P-gp homologues show conservation of about 60% of all TMD residues (Mandal *et al.* 2012). Dey and coworkers mutated non-conserved residues in the TMDs in order to identify residues involved in binding of *cis*-flupentixol. These residues were found to be exclusively located in TMD2 (Fig. 7A, B) in contrast to those identified for a number of paradigmatic P-gp substrates – including propafenones, verapamil, and vinblastine. We here report that the  $\Delta Y490$  mutant is rescued more efficiently than the  $\Delta Y1133$  mutant, which requires approximately fourfold higher pharmacochaperone concentration for rescue (Fig. 7C, D). *cis*-Flupentixol interacts with residues located in TM helices 9, 10, 11, and 12. Formation of the binding site around the ligand stabilizes the positions of these helices, thereby defining the spatial orientation of ICL4. We posit that this stabilization of the helical bundle of TMD2 promotes interaction with NBD1. Folding correction of the NBD2 mutant occurs at much higher compound concentrations and is likely due to a global stabilization effect.

In conclusion, the difference in the rescue of P-gp interface mutants with *cis*-flupentixol reflects the asymmetric binding properties of this P-gp modulator. In contrast, several different active site compounds aid in correct positioning of both intracellular loops. Thereby,

they promote the engagement of coupling helices by a groove, which is present on the surface of either of the two NBDs and which is oriented toward the TMD. Correct folding of the NBDs is required for proper positioning of ICLs and, therefore, the NBDs act as proteinaceous chaperones in the folding of the wild-type protein. Conversely, the TMDs also stabilize the NBD dimer. In the case of NBD misfolding the likelihood of ICLs and TMDs to adopt their fully folded conformation is decreased due to the loss of NBD-assisted positioning. In the latter case, active site compounds aid in correct positioning of intracellular loops, thereby enabling the protein to reach a conformation which is required to pass folding and trafficking checkpoints.

## Acknowledgements

We would like to thank Saibal Dey for sharing results prior to publication and for providing us with *cis*-flupentixol.

## Author Contributions

Participated in research design: Spork, Chiba. Conducted experiments: Spork, Sohail, Stockner. Contributed new reagents or analytic tools: Schmid, Ecker. Performed data analysis: Spork, Chiba, Stockner. Wrote or contributed to writing of the manuscript: Spork, Freissmuth, Chiba.

## Disclosure

None declared.

## References

- Bodzioch M, Orso E, Klucken J, Langmann T, Bottcher A, Diederich W, *et al.* (1999). The gene encoding ATP-binding cassette transporter 1 is mutated in Tangier disease. *Nat Genet* 22: 347–351.
- Burgen AS (1981). Conformational changes and drug action. *Fed Proc* 40: 2723–2728.
- Changeux JP, Thiery J, Tung Y, Kittel C (1967). On the cooperativity of biological membranes. *Proc Natl Acad Sci USA* 57: 335–341.
- Cheong N, Madesh M, Gonzales LW, Zhao M, Yu K, Ballard PL, *et al.* (2006). Functional and trafficking defects in ATP binding cassette A3 mutants associated with respiratory distress syndrome. *J Biol Chem* 281: 9791–9800.
- Chiba P, Burghofer S, Richter E, Tell B, Moser A, Ecker G (1995). Synthesis, pharmacologic activity, and structure-activity relationships of a series of propafenone-related modulators of multidrug resistance. *J Med Chem* 38: 2789–2793.

- Chiba P, Rebitzer S, Richter E, Hitzler M, Ecker G (1998). Synthesis and pharmacological activity of the stereoisomers of GP-88, a propafenone-type modulator of multidrug resistance. *Bioorg Med Chem Lett* 8: 829–832.
- Chiba P, Freissmuth M, Stockner T (2014). Defining the blanks–pharmacochaperoning of SLC6 transporters and ABC transporters. *Pharmacol Res* 83: 63–73.
- Delaunay JL, Durand-Schneider AM, Delautier D, Rada A, Gautherot J, Jacquemin E, et al. (2009). A missense mutation in ABCB4 gene involved in progressive familial intrahepatic cholestasis type 3 leads to a folding defect that can be rescued by low temperature. *Hepatology* 49: 1218–1227.
- Denning GM, Anderson MP, Amara JF, Marshall J, Smith AE, Welsh MJ (1992). Processing of mutant cystic fibrosis transmembrane conductance regulator is temperature-sensitive. *Nature* 358: 761–764.
- Donmez Cakil Y, Khunweeraphong N, Parveen Z, Schmid D, Artaker M, Ecker GF, et al. (2014). Pore-exposed tyrosine residues of P-glycoprotein are important hydrogen-bonding partners for drugs. *Mol Pharmacol* 85: 420–428.
- Du K, Lukacs GL (2009). Cooperative assembly and misfolding of CFTR domains in vivo. *Mol Biol Cell* 20: 1903–1915.
- Farrell PM (2008). The prevalence of cystic fibrosis in the European Union. *J Cyst Fibros* 7: 450–453.
- Gautherot J, Durand-Schneider AM, Delautier D, Delaunay JL, Rada A, Gabillet J, et al. (2012). Effects of cellular, chemical, and pharmacological chaperones on the rescue of a trafficking-defective mutant of the ATP-binding cassette transporter proteins ABCB1/ABCB4. *J Biol Chem* 287: 5070–5078.
- Gottesman MM, Pastan I (1993). Biochemistry of multidrug resistance mediated by the multidrug transporter. *Annu Rev Biochem* 62: 385–427.
- Hartley JL, Temple GF, Brasch MA (2000). DNA cloning using in vitro site-specific recombination. *Genome Res* 10: 1788–1795.
- Hashimoto K, Uchiumi T, Konno T, Ebihara T, Nakamura T, Wada M, et al. (2002). Trafficking and functional defects by mutations of the ATP-binding domains in MRP2 in patients with Dubin-Johnson syndrome. *Hepatology* 36: 1236–1245.
- Hayashi H, Takada T, Suzuki H, Akita H, Sugiyama Y (2005). Two common PFIC2 mutations are associated with the impaired membrane trafficking of BSEP/ABCB11. *Hepatology* 41: 916–924.
- Hirouchi M, Suzuki H, Itoda M, Ozawa S, Sawada J, Ieiri I, et al. (2004). Characterization of the cellular localization, expression level, and function of SNP variants of MRP2/ABCC2. *Pharm Res* 21: 742–748.
- Hoof T, Demmer A, Hadam MR, Riordan JR, Tummeler B (1994). Cystic fibrosis-type mutational analysis in the ATP-binding cassette transporter signature of human P-glycoprotein MDR1. *J Biol Chem* 269: 20575–20583.
- Imai Y, Nakane M, Kage K, Tsukahara S, Ishikawa E, Tsuruo T, et al. (2002). C421A polymorphism in the human breast cancer resistance protein gene is associated with low expression of Q141K protein and low-level drug resistance. *Mol Cancer Ther* 1: 611–616.
- Iram SH, Cole SP (2012). Mutation of Glu521 or Glu535 in cytoplasmic loop 5 causes differential misfolding in multiple domains of multidrug and organic anion transporter MRP1 (ABCC1). *J Biol Chem* 287: 7543–7555.
- Jin MS, Oldham ML, Zhang Q, Chen J (2012). Crystal structure of the multidrug transporter P-glycoprotein from *Caenorhabditis elegans*. *Nature* 490: 566–569.
- Kerem B, Rommens JM, Buchanan JA, Markiewicz D, Cox TK, Chakravarti A, et al. (1989). Identification of the cystic fibrosis gene: genetic analysis. *Science* 245: 1073–1080.
- Kleizen B, van Vlijmen T, de Jonge HR, Braakman I (2005). Folding of CFTR is predominantly cotranslational. *Mol Cell* 20: 277–287.
- Langer T, Eder M, Hoffmann RD, Chiba P, Ecker GF (2004). Lead identification for modulators of multidrug resistance based on in silico screening with a pharmacophoric feature model. *Arch Pharm (Weinheim)* 337: 317–327.
- Le Saux O, Fulop K, Yamaguchi Y, Ilias A, Szabo Z, Brampton CN, et al. (2011). Expression and in vivo rescue of human ABCC6 disease-causing mutants in mouse liver. *PLoS ONE* 6: e24738.
- Lee JY, Kinch LN, Borek DM, Wang J, Wang J, Urbatsch IL, et al. (2016). Crystal structure of the human sterol transporter ABCG5/ABCG8. *Nature* 533: 561–564.
- Loo TW, Clarke DM (1994). Prolonged association of temperature-sensitive mutants of human P-glycoprotein with calnexin during biogenesis. *J Biol Chem* 269: 28683–28689.
- Loo TW, Clarke DM (1997). Correction of defective protein kinesis of human P-glycoprotein mutants by substrates and modulators. *J Biol Chem* 272: 709–712.
- Loo TW, Clarke DM (1998). Nonylphenol ethoxylates, but not nonylphenol, are substrates of the human multidrug resistance P-glycoprotein. *Biochem Biophys Res Comm* 247: 478–480.
- Loo TW, Clarke DM (2013). Drug rescue distinguishes between different structural models of human P-glycoprotein. *Biochemistry* 52: 7167–7169.
- Loo TW, Clarke DM (2014). Tariquidar inhibits P-glycoprotein drug efflux but activates ATPase activity by blocking transition to an open conformation. *Biochem Pharmacol* 92: 558–566.
- Loo TW, Clarke DM (2015). The Transmission Interfaces Contribute Asymmetrically to the Assembly and Activity of Human P-glycoprotein. *J Biol Chem* 290: 16954–16963.



- Loo TW, Bartlett MC, Clarke DM (2005). Rescue of folding defects in ABC transporters using pharmacological chaperones. *J Bioenerg Biomembr* 37: 501–507.
- Loo TW, Bartlett MC, Clarke DM (2013). Human P-glycoprotein contains a greasy ball-and-socket joint at the second transmission interface. *J Biol Chem* 288: 20326–20333.
- Machamer CE, Rose JK (1988). Vesicular stomatitis virus G proteins with altered glycosylation sites display temperature-sensitive intracellular transport and are subject to aberrant intermolecular disulfide bonding. *J Biol Chem* 263: 5955–5960.
- Maki N, Dey S (2006). Biochemical and pharmacological properties of an allosteric modulator site of the human P-glycoprotein (ABCB1). *Biochem Pharmacol* 72: 145–155.
- Maki N, Hafkemeyer P, Dey S (2003). Allosteric modulation of human P-glycoprotein. Inhibition of transport by preventing substrate translocation and dissociation. *J Biol Chem* 278: 18132–18139.
- Mandal D, Moitra K, Ghosh D, Xia D, Dey S (2012). Evidence for modulatory sites at the lipid-protein interface of the human multidrug transporter P-glycoprotein. *Biochemistry* 51: 2852–2866.
- Matsuo H, Takada T, Ichida K, Nakamura T, Nakayama A, Ikebuchi Y, *et al.* (2009). Common defects of ABCG2, a high-capacity urate exporter, cause gout: a function-based genetic analysis in a Japanese population. *Sci Transl Med* 1: 5ra11.
- Nicklisch SC, Rees SD, McGrath AP, Gokirmak T, Bonito LT, Vermeer LM, *et al.* (2016). Global marine pollutants inhibit P-glycoprotein: environmental levels, inhibitory effects, and cocrystal structure. *Sci Adv* 2: e1600001.
- Parveen Z, Stockner T, Bentele C, Pferschy S, Kraupp M, Freissmuth M, *et al.* (2011). Molecular dissection of dual pseudosymmetric solute translocation pathways in human P-glycoprotein. *Mol Pharmacol* 79: 443–452.
- Pedemonte N, Lukacs GL, Du K, Caci E, Zegarra-Moran O, Galiotta LJ, *et al.* (2005). Small-molecule correctors of defective DeltaF508-CFTR cellular processing identified by high-throughput screening. *J Clin Invest* 115: 2564–2571.
- Plass JR, Mol O, Heegsma J, Geuken M, de Bruin J, Elling G, *et al.* (2004). A progressive familial intrahepatic cholestasis type 2 mutation causes an unstable, temperature-sensitive bile salt export pump. *J Hepatol* 40: 24–30.
- Pleban K, Kopp S, Csaszar E, Peer M, Hrebicek T, Rizzi A, *et al.* (2005). P-glycoprotein substrate binding domains are located at the transmembrane domain/transmembrane domain interfaces: a combined photoaffinity labeling-protein homology modeling approach. *Mol Pharmacol* 67: 365–374.
- Polgar O, Robey RW, Morisaki K, Dean M, Michejda C, Sauna ZE, *et al.* (2004). Mutational analysis of ABCG2: role of the GXXXG motif. *Biochemistry* 43: 9448–9456.
- Rabeh WM, Bossard F, Xu H, Okiyoneda T, Bagdany M, Mulvihill CM, *et al.* (2012). Correction of both NBD1 energetics and domain interface is required to restore DeltaF508 CFTR folding and function. *Cell* 148(1–2): 150–163.
- Rees DC, Johnson E, Lewinson O (2009). ABC transporters: the power to change. *Nat Rev Mol Cell Biol* 10: 218–227.
- Riordan JR, Rommens JM, Kerem B, Alon N, Rozmahel R, Grzelczak Z, *et al.* (1989). Identification of the cystic fibrosis gene: cloning and characterization of complementary DNA. *Science* 245: 1066–1073.
- Rust S, Rosier M, Funke H, Real J, Amoura Z, Piette JC, *et al.* (1999). Tangier disease is caused by mutations in the gene encoding ATP-binding cassette transporter 1. *Nat Genet* 22: 352–355.
- Schmid D, Ecker G, Kopp S, Hitzler M, Chiba P (1999). Structure-activity relationship studies of propafenone analogs based on P-glycoprotein ATPase activity measurements. *Biochem Pharmacol* 58: 1447–1456.
- Shapiro AB, Ling V (1997). Positively cooperative sites for drug transport by P-glycoprotein with distinct drug specificities. *Eur J Biochem* 250: 130–137.
- Singaraja RR, Visscher H, James ER, Chroni A, Coutinho JM, Brunham LR, *et al.* (2006). Specific mutations in ABCA1 have discrete effects on ABCA1 function and lipid phenotypes both in vivo and in vitro. *Circ Res* 99: 389–397.
- Sorenson B, Suetani RJ, Williams MJ, Bickley VM, George PM, Jones GT, *et al.* (2013). Functional rescue of mutant ABCA1 proteins by sodium 4-phenylbutyrate. *J Lipid Res* 54: 55–62.
- Stockner T, de Vries SJ, Bonvin AM, Ecker GF, Chiba P (2009). Data-driven homology modelling of P-glycoprotein in the ATP-bound state indicates flexibility of the transmembrane domains. *FEBS J* 276: 964–972.
- Thompson CA (2008). First drug approved for treatment of phenylketonuria. *Am J Health-Syst Pharm* 65: 100.
- Tornovsky S, Crane A, Cosgrove KE, Hussain K, Lavie J, Heyman M, *et al.* (2004). Hyperinsulinism of infancy: novel ABCC8 and KCNJ11 mutations and evidence for additional locus heterogeneity. *J Clin Endocrinol Metab* 89: 6224–6234.
- Wang Y, Loo TW, Bartlett MC, Clarke DM (2007). Modulating the folding of P-glycoprotein and cystic fibrosis transmembrane conductance regulator truncation mutants with pharmacological chaperones. *Mol Pharmacol* 71: 751–758.

## Supporting Information

Additional Supporting Information may be found online in the supporting information tab for this article:



**Figure S1.** The positions of tyrosine 490 in NBD1 (orange), tyrosine 1133 in NBD2 (red), and coupling helices (CH) of ICLs2 and 4 (CH2, CH4) are depicted in a homology model of human P-gp (template *M. musculus* P-gp (PDB ID: 4XWK)).

**Figure S2.** Positions of residues Y490 (orange) and Y1133 (red) as well as residues, which were previously

found to be photolabeled by intrinsically photoactive propafenone analogs are indicated in a homology model of human P-gp (template *M. musculus* P-gp (PDB ID: 4XWK)).

**Table S1.** SNPs in ICLs and NBDs of human ABC proteins.